Journal of Hazardous Materials 196 (2011) 52–58

Contents lists available at SciVerse ScienceDirect

Journal of Hazardous Materials

journal homepage: www.elsevier.com/locate/jhazmat

Improvement of gaseous pollutant photocatalysis with WO_3/TiO_2 heterojunctional-electrical layered system

Yuan Liu, Changsheng Xie*, Huayao Li, Hao Chen, Tao Zou, Dawen Zeng

State Key Laboratory of Material Processing and Die & Mould Technology, Nanomaterials and Smart Sensors Laboratory, Department of Materials Science and Engineering, Huazhong University of Science and Technology, Wuhan 430074, PR China

ARTICLE INFO

Article history:
Received 23 June 2011
Received in revised form 27 August 2011
Accepted 29 August 2011
Available online 2 September 2011

Keywords:
Holes enrichment
Photocatalysis
Gas phase
Synergistic effect
Thermodynamics

ABSTRACT

Since the photogenerated holes play a much more important role than electrons in gas-phase photocatalysis, it is better to enrich the holes in the surface of a material system. Here, a novel [interdigital electrode/WO_3/TiO_2] heterojunctional-electrical layered (HEL) system is proposed to realize this attempt. The HEL system consists of interdigital electrode, WO_3 layer and TiO_2 layer, and they are orderly printed onto the alumina substrate from bottom to top using the technology of screen printing. It is surprise that the synergistic effect of layered heterojunction and external low bias can strengthen the separation of electron–hole pairs in both TiO_2 and WO_3, and enrich the TiO_2 surface layer with photogenerated holes to degrade the gaseous pollutants. In comparison with the pure TiO_2 film, a 6-fold enhancement in photocatalytic activity was observed using the HEL system by applying a very low bias of 0.2 V. Furthermore, the results also showed that the remarkable improvement could not be obtained when either the WO_3 layer or the low external bias was absent.

1. Introduction

Photocatalytic technology is an effective pathway for solving the problems of energy crisis and environmental pollution [1,2]. TiO_2 semiconductor has been frequently investigated owing to its high oxidation ability, inexpensive, nontoxicity, and chemical stability. However, as a photocatalyst, the relatively high rate of electron–hole recombination often results in a low quantum yield and poor efficiency of photocatalytic reactions [3–6].

Among the ways of enhancing the separation of photogenerated charge carriers, constructing heterojunction structures [7–9] and applying external biases [10–12] are both effective methods to improve the photocatalytic activity of TiO_2. However, the two methods suffer severe constraints when they are applied in the gas-phase photocatalysis, respectively.

With regard to the heterojunction structure, it is generally prepared by the simple physical mixing, such as ball milling and sol–gel method, which produces a random mixture of different nanoparticles [6,13]. Thus far, WO_3 coupling has been widely studied to improve the photocatalytic performances of TiO_2, since WO_3 has the suitable matching band potential to serve as electron accepting species. However, in the confirmation of degradation of gaseous volatile organic chemicals (VOCs), the photocatalytic activity of TiO_2/WO_3 composite is not obviously enhanced than that of pure TiO_2, and it is even weakened with the increased amount of WO_3 [14–16]. Recently, both theoretical and experimental studies indicate that the reduction reactions initiated by the electrons are much less effective than the oxidation reactions conducted by the holes which can induce complete decomposition of gaseous pollutants at room temperature [17–21]. Therefore, in the mixed WO_3/TiO_2 composite, WO_3 as an electron accepting species not only poorly contributes to the gaseous photocatalysis, but also reduces the surface area between TiO_2 and the gaseous pollutants. Hence, the presence of WO_3 can only be accounted for enhancing the photocatalytic activity, when its content is significantly less than TiO_2 [13,16]. As a result, the interface of the heterojunction for charge separation cannot be sufficiently utilized in the mixed form. It can be seen that the layered structure with the hole accepting species facing the VOCs may be more promising than the mixed form.

With regard to the application of an external bias voltage, the applied bias on the catalyst can draw the photogenerated electrons away via the external circuit, leaving holes for mineralization of organic pollutants by their oxidation, which is the main characteristic of photoelectrocatalytic (PEC) process [22,23]. Until now, the PEC degradation researches are mainly carried out in aqueous solution, but rarely in gas phase. This is because that catalyst efficiency of traditional TiO_2 was improved with very high bias (~100 V), which needed special potentiostat or voltage booster and consumed more electric energy [24,25]. In the view of low carbon economy, it is obviously more worthwhile to deal with the improvement by applying a relative low bias (<0.5 V).

* Corresponding author. Tel.: +86 27 8755 6544; fax: +86 27 8754 3778.
E-mail address: csxie@mail.hust.edu.cn (C. Xie).

0304-3894/$ – see front matter © 2011 Elsevier B.V. All rights reserved.
doi:10.1016/j.jhazmat.2011.08.067

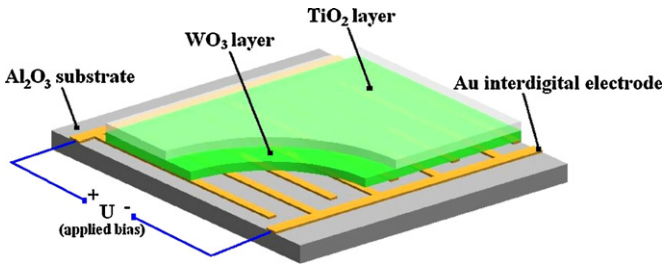

Fig. 1. Schematic diagram of the [interdigital electrode/WO_3/TiO_2] HEL system (Al_2O_3 substrate, Au interdigital electrode layer, WO_3 layer and TiO_2 layer from bottom to top).

Taking the above into consideration, we firstly introduce a new strategy for sufficiently utilizing the photogenerated holes by combining the two methods in one photocatalytic system for gas-phase application, which is defined as heterojunctional-electrical layered (HEL) system. When a very low bias is needed and the holes can be enriched in the surface layer, this system can well settle the bottlenecks of the two methods applied in the gas-phase photocatalysis, respectively. In this study, the system consists of interdigital electrode, WO_3 layer and TiO_2 layer, and the three functional layers are laminated from bottom to top using the technique of screen printing (schematically shown in Fig. 1). Based on the experimental results, the charge transportation in terms of the thermodynamics in this system is discussed in detail. We expect that the proposed photocatalytic model for the gas phase application may open a new avenue for the design of high efficient photocatalyst with a powerful oxidative ability, and give a novel sight in the combination of heterojunctional photocatalytic and PEC techniques.

2. Experimental

2.1. Materials

TiO_2 (Degussa P25, average grain size: 30 nm), WO_3 (Tianjin Kermel Chemical Reagent Co. Ltd., China, average grain size: 80 nm) and other chemicals used in the experiment were of analytically pure grade. All of them were used as received without any pretreatment.

2.2. Samples preparation and characterization

There are many methods to prepare semiconductor film, e.g., sol–gel, sputter deposition, coprecipitation, etc. However, few works are reported to investigate the photocatalyst film by screen printing technique, which is a well-known process in the ceramic industry [26]. In this study, the preparation of [interdigital electrode/TiO_2/WO_3] HEL system was based on the screen-printing technique. The designed sample is schematically shown in Fig. 1.

Firstly, the chemical powder (TiO_2 or WO_3) and a certain amount of organic carrier (a 55:30:10:4:1 wt% combination of terpineol, butyl carbitol, di-*n*-butyl phthalate, span 85, and ethyl-cellulose) were mixed in a 7:3 wt ratio. All of them were put into the agate ball milling tank. After ball milling for 4 h at the speed of 300 rpm, the suitable pastes used for the process of screen printing were obtained. Additional details of paste preparation are available in our previous report [27].

Secondly, the WO_3 paste was printed onto the Au interdigital electrode which had been preprinted on the alumina substrate (Zhuhai Yueke Jinghua Electronic Ceramics CO. LTD., China). After drying, the TiO_2 paste was printed onto the WO_3 layer. The thickness of each photocatalyst layer was about 10 μm, which could be controlled by the screen printing machine. Then, the samples were preheated at 200 °C for 15 min to eliminate the organic carrier. In the end, the samples were sintered at 550 °C for 2 h. Following the above procedures, the [interdigital electrode/WO_3/TiO_2] HEL system could be successfully obtained, in which the Al_2O_3 substrate, interdigital electrode, WO_3 layer and TiO_2 layer were laminated from bottom to top. Furthermore, the [interdigital electrode/TiO_2/WO_3], [interdigital electrode/TiO_2/TiO_2], [interdigital electrode/WO_3/WO_3] parallel samples were also prepared by the same method. The prepared samples were characterized by field-emission scanning electron microscopy (FSEM, Sirion 200, FEI), X-ray diffraction (XRD, X'Pert PRO, PANalytical B.V.), UV–vis DRS spectra (Lambda 35, PerkinElmer) and photoluminescence spectra (PL, USB2000-FLG Ocean Optics Spectrometer).

2.3. Evaluation of photocatalytic activity

Photocatalytic activities of the prepared samples under UV light were evaluated by the following method. The samples could be installed in a gas reactor system. The total volume of this reactor was 825 ml. The whole printed area of the photocatalytic film was 50 mm × 50 mm, which was irradiated by a flat-type LED-light (Shenzhen Ti-times Electronics Co. Ltd., China, wavelength: 365 ± 5 nm). The power of the light irradiated to the surface of photocatalytic sample was 5 mW/cm^2.

In our experiments, the gaseous toluene was used as a model pollutant, which was a persistent indoor volatile harmful gas. Prior to a test, 250 ppm toluene gas (dry air and toluene mixture) was allowed to enter the reactor until the toluene reached adsorption and desorption equilibrium with the catalyst and the reactor. The initial concentration of toluene was 250 ppm (±5 ppm). Each experiment was lasted for 30 min. The analysis of toluene, carbon dioxide concentration in the reactor was conducted on line with a Photoacoustic IR Multigas Monitor (Model 1412; INNOVA Air Tech Instruments).

The photocatalytic activity of different samples can be quantitatively evaluated by comparing the apparent reaction rate constants. In a heterogeneous solid–gas reaction, the photocatalytic degradation of toluene is a pseudo-first-order reaction, and its kinetic equation may be expressed as follows [28,29]:

$$\ln \frac{C_0}{C_t} = kt$$

where k is the apparent rate constant, C_0 and C_t are the initial and the reaction concentration of toluene, respectively.

2.4. Measurements of photoelectric response

To evaluate the separation ability of photoexcited electron–hole pairs in the semiconductor materials, photoelectric property measurement was performed. Photocurrent characterization was carried out with a flat-type LED-light (365 ± 5 nm) as the UV light source. The light intensity was about 5 mW/cm^2. The platform was developed independently by our laboratory, which had the testing photocurrent range in 10^{-8} to 10^{-3} A. In this study, the photocurrent was measured in the dry air and the amplitude illuminated for 270 s was chosen as a parameter to assess the photoelectric response of the material. The detailed descriptions of the platform and the test procedures can refer to our previous work [30,31].

3. Results and discussion

3.1. Film characteristics

The detailed descriptions of the prepared samples are shown in Table 1. Designations are used in the following discussions. [Interdigital electrode/WO_3/TiO_2], [interdigital

Table 1
Designations and structure descriptions of the as-prepared samples.

Sample	[IE/WO_3/TiO_2]	[IE/TiO_2/WO_3]	[IE/TiO_2/TiO_2]	[IE/WO_3/WO_3]
Designation	S-W/T	S-T/W	S-T	S-W
Substrate	Al_2O_3 substrate printed with Au interdigital electrode			
Underlayer	WO_3	TiO_2	TiO_2	WO_3
Toplayer	TiO_2	WO_3		
Film thickness	20 μm in total (toplayer = underlayer = 10 μm)		20 μm	20 μm

IE: interdigital electrode.

electrode/TiO_2/WO_3], [interdigital electrode/TiO_2/TiO_2] and [interdigital electrode/WO_3/WO_3] samples are called S-W/T, S-T/W, S-T and S-W, respectively.

The surface morphologies and phase components of the S-W/T prepared by the screen-printing technique are shown in Fig. 2. The SEM photograph in Fig. 2a shows the cross-sectional morphology of the WO_3/TiO_2 layered structure. The printed film is about 20 μm in thickness, in which the TiO_2 and WO_3 layers are both about 10 μm. An apparent interface between two layers is observed, indicating that it is two-layer type heterojunction and is different from the mixture type in a composite system. From the insert of Fig. 2a, we can see that the film has lots of micro-holes, which are formed due to volatilization of organic component during the heat-treatment process and originated from agglomerated structures in the screen printing paste. These micro-holes let the film to have a good absorption property for the light and gaseous chemicals [12]. Moreover,

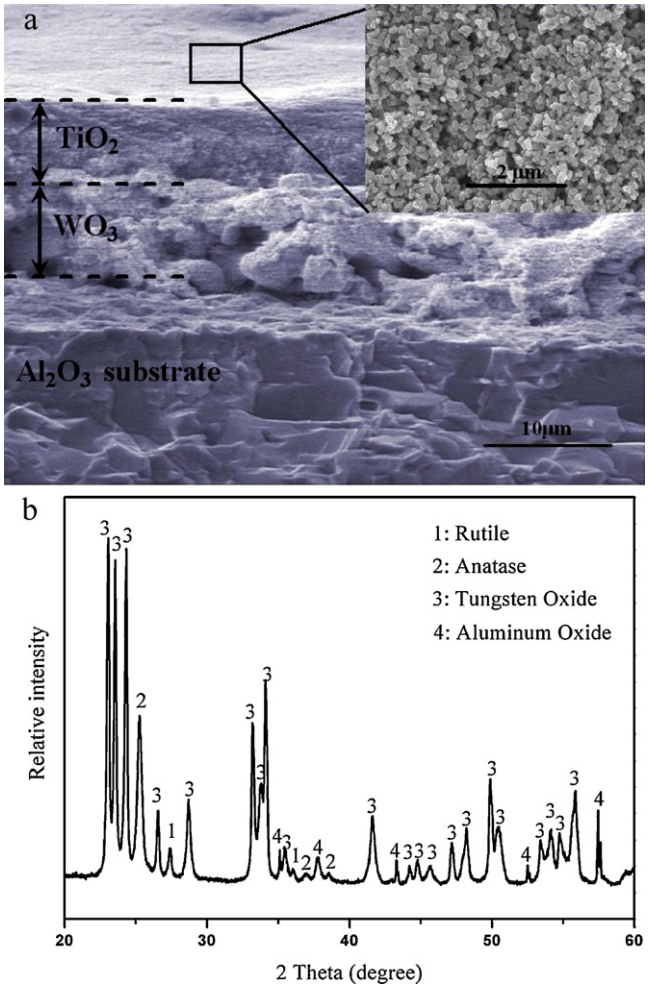

Fig. 2. (a) A typical cross-sectional view SEM image of the as-prepared S-W/T sample, the inset in showing the top surface SEM image of it; (b) X-ray diffraction patterns of the as-prepared S-W/T sample.

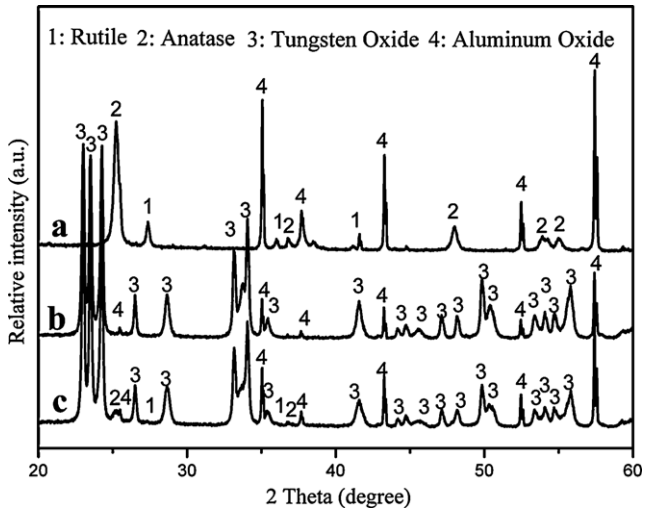

Fig. 3. X-ray diffraction patterns of as-prepared (a) S-T, (b) S-W and (c) S-T/W parallel samples.

sintering neck as an important structure for composite photocatalyst is formed between two contacted grains. It is considered as the chemically bounded interface caused by ionic thermal diffusion to allow the smooth charge transfer [9,14,32].

The XRD patterns in Fig. 2b illustrate that the phase components of the S-W/T sample are not changed after the heat-treatment at 550 °C. No other phases are found in the sample, suggesting that there is no appreciable chemical reaction between TiO_2 and WO_3. The S-T/W, S-T, S-W samples have the similar results, as shown in Fig. 3.

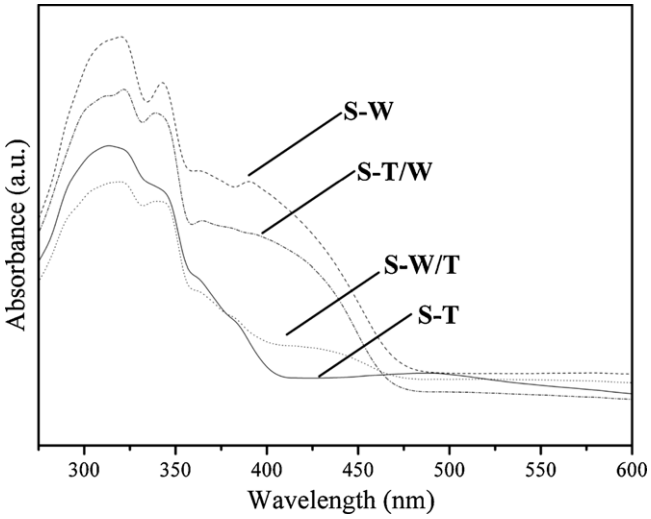

Fig. 4. UV–vis diffuses reflectance spectra of the as-prepared S-T, S-W, S-W/T and S-T/W samples.

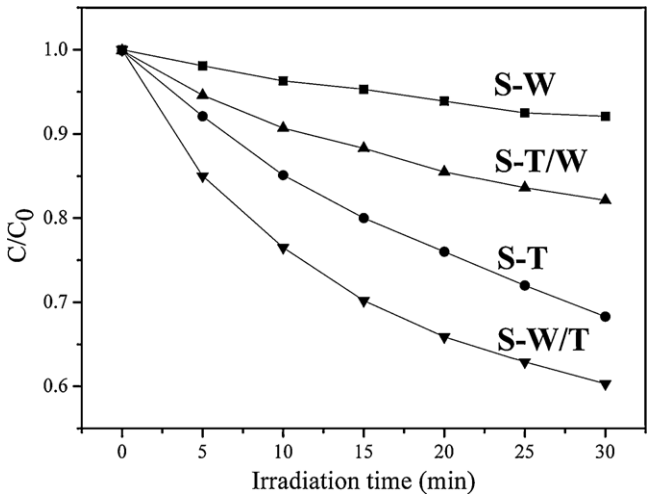

Fig. 5. The comparisons of degradation rate among the samples without bias under UV-light (365 nm) irradiation.

Fig. 4 indicates the UV–vis diffuse reflectance spectral of the four samples. The S-T and S-W samples exhibit absorption below 390 and 450 nm, which correspond to their absorption edges (E_g = 3.2 eV for TiO_2 and E_g = 2.8 eV for WO_3), respectively. Furthermore, the S-W sample has higher absorption intensity than S-T sample in both UV and visible regions. For coupled films, the S-W/T and S-T/W samples show the similar absorption profiles as their toplayers. In addition, S-W/T sample has higher absorption intensity than S-T sample in the visible region. This suggested that the visible light could penetrate the TiO_2 toplayer to excite the WO_3 underlayer because of a lot of micro-holes in the film. To simplify the following discussion about the charge separation, the UV (365 nm) light is used for the photocatalytic activity and photocurrent tests, since the S-W/T and S-T samples have the same absorption intensity at this wavelength.

3.2. Photocatalytic activity without bias

The photocatalytic activity of the as-prepared samples is evaluated by the photocatalytic degradation of toluene in air. Blank experiments indicate that the photocatalytic reactions do not take place in the absence of either photocatalysts or UV light. Fig. 5 shows the photocatalytic removal of toluene versus irradiation time and the apparent rate constants are 3.03, 7.39, 13.57 and 20.04 × 10^{-3} min^{-1} for the S-W, S-T/W, S-T and S-W/T, respectively.

Based on Fig. 5, the order of photocatalytic activity is S-W < S-T/W < S-T < S-W/T. The S-W sample has a much lower photocatalytic activity than S-T sample, although it has higher absorption intensity. The possible reason for the low rate constant of S-W sample is associated with the poor photocatalytic activity of WO_3. The WO_3 has a narrow band of 2.8 eV and a low potential of the conduction band (CB) bottom (−5.24 eV versus Vacuum) [33]. So that the photo-generated electrons do not have enough reducibility to react with the molecule oxygen at room temperature, expressed as the following equation [34]:

$$O_2(g) + e^- \rightarrow O_2^-(ad), \quad -4.216\,eV\ versus\ Vacuum \tag{1}$$

It is generally considered that the CB level of a semiconductor should be more negative than the potential for the single-electron reduction of oxygen in order to allow efficient consumption of photoexcited electrons and subsequent oxidative decomposition of organic compounds by holes to proceed in air [34]. Otherwise, photoexcited electrons probably recombine with photogenerated holes, resulting in the high probability of the fast recombination of the photogenerated electron–hole pairs in the WO_3 film. In a word, the photoexcited electrons of WO_3 cannot be used for one-electron chemical reaction effectively at room temperature. In addition, the recombination of the photogenerated electron–hole pairs is further enhanced. This fact lets us to believe that WO_3 is unsuitable for achieving the efficient oxidative decomposition of organic compounds in air.

Fig. 6 shows the PL spectra of S-W and S-T samples under excitation at 300 nm. The PL signals of semiconductor materials result from the recombination of photoinduced charge carriers. In general, the lower PL intensity indicates the lower recombination rate of photoinduced electron–hole pairs and the higher photocatalytic activity of semiconductors. As can be seen in Fig. 6, TiO_2 shows the lower and narrower PL intensity than WO_3. Therefore, the PL results in Fig. 6 are consistent with the photocatalytic activity of the samples in Fig. 5. It is concluded that the rapid recombination of photogenerated electron–hole pairs is directly harmful to the photocatalytic efficiency.

Importantly, it is noted that the S-W/T sample exhibits the best photocatalytic activity, though the S-W/T sample has the same absorption of UV light as the S-T sample. Therefore, the increase in the photocatalytic activity can be attributed to the charge separation between TiO_2 and WO_3. A mechanistic scheme of the charge separation for the S-W/T system is shown in Fig. 7. Both TiO_2 and WO_3 are *n*-type semiconductor with suitable bandgap energies, strongly absorbing UV light. Upon photon-excitation, electron–hole pairs are generated in each semiconductor film, expressed as the process 1 and process 2, respectively:

$$TiO_2 + h\nu \xrightarrow{1} e_{TiO_2}{}^- + h_{TiO_2}{}^+ \tag{2}$$

$$WO_3 + h\nu \xrightarrow{2} e_{WO_3}{}^- + h_{WO_3}{}^+ \tag{3}$$

The valence band (VB) edges of TiO_2 and WO_3 are situated at −7.41 and −7.94 eV versus Vacuum level, respectively. The CB edge of WO_3 (−5.24 eV) is much lower than that of TiO_2 (−4.21 eV) [33]. In terms of the thermodynamics, electrons can flow into the WO_3 underlayer, while holes oppositely diffuse into the TiO_2 toplayer, expressed as the process 3 and process 4, respectively:

$$e_{TiO_2}{}^- \xrightarrow{3} e_{WO_3}{}^- \tag{4}$$

$$h_{WO_3}{}^+ \xrightarrow{4} h_{TiO_2}{}^+ \tag{5}$$

So far, variety of the TiO_2/WO_3 coupled systems have been widely reported. As shown in Fig. 7a, only the above four processes

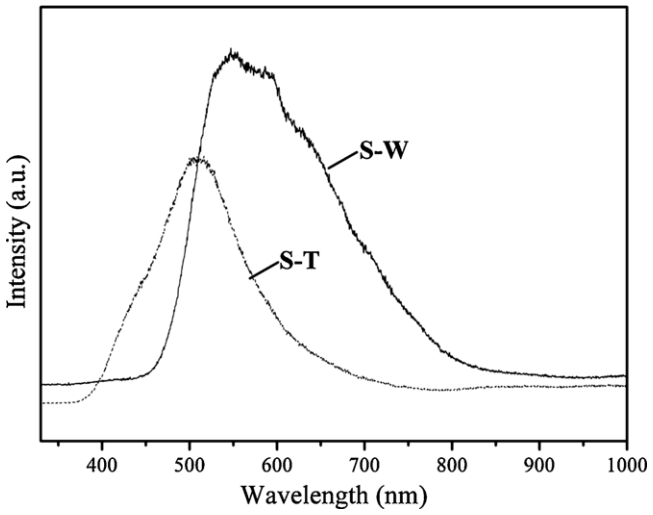

Fig. 6. Excitation dependent PL of S-W and S-T samples.

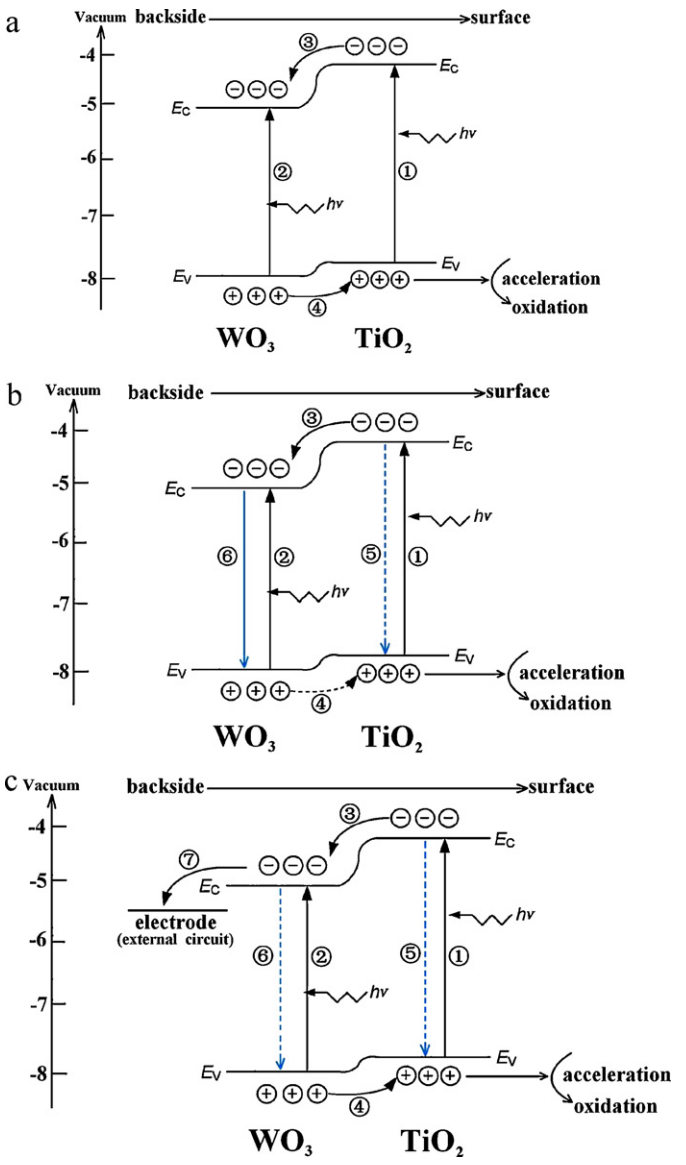

Fig. 7. Schematic diagram for energy band matching and flow of electrons and holes in the S-W/T system. (a) The recombination processes are generally ignored in previous reports. (b) No bias is supplied. (c) A low bias of 0.2 V is supplied. Note that the process is drawn as a dotted line when it is inhibited.

were considered to discuss the charge transfer in the correlative references. Nevertheless, the process of electron–hole recombination that is directly related to the photocatalytic ability was not carefully concerned. The recombination of the photogenerated electron–hole pairs in the TiO_2 layer and WO_3 layer is expressed as the process 5 and process 6, respectively:

$$e_{TiO_2}{}^{-} + h_{TiO_2}{}^{+} \xrightarrow{5} \text{energy} \quad (6)$$

$$e_{WO_3}{}^{-} + h_{WO_3}{}^{+} \xrightarrow{6} \text{energy} \quad (7)$$

As is well known, in n-type semiconductor, the mobility of the electrons is much higher than that of the holes [35,36]. When the TiO_2/WO_3 coupled system is illuminated by the UV-light, the photogenerated electrons in the CB of TiO_2 would be very rapidly and easily transferred to the CB of WO_3 (process 3). However, the process 4, that the holes move in the opposite direction from the electrons and are trapped in the TiO_2, should be slow and inefficient. That is to say, the WO_3 would be accumulated with more electrons, but the holes of WO_3 are not efficiently separated, resulting in the large recombination probability (process 6). Then, the transportation of the holes from the valance of WO_3 to that of TiO_2 is further suppressed (process 4). As a result, the higher photocatalytic activity of the TiO_2/WO_3 coupled films is just due to the lower recombination rate in the TiO_2 toplayer (process 5). Thus, the above discussions can deeply explain the higher photocatalytic activity of the WO_3/TiO_2 layered film. The detailed production, recombination and transportation processes of charge carriers are schematically illustrated in Fig. 7b.

Table 2
The apparent rate constants and the amount of evolved CO_2 when the S-T and S-W/T samples are unbiased and 0.2 V biased.

Samples	Rate constant (10^{-3} min^{-1})		Evolved CO_2 (ppm)	
	Unbiased	0.2 V biased	Unbiased	0.2 V biased
S-T	13.57	13.88	458	469
S-W/T	20.04	84.73	609	1186

For the reverse coupled TiO_2/WO_3 film (S-T/W sample), the WO_3 toplayer accumulated with electrons gets in touch with the gaseous toluene. As noticed in Fig. 5, the photocatalytic activity of the S-T/W sample is higher than S-W sample but lower than S-T sample. This proves that the contribution of the electrons to the photocatalytic activity does not have so much as the holes. It should be also mentioned that the film prepared by the screen-printing method, as indicated in the insert of Fig. 2a, is micro-porous. Therefore, a portion of gaseous toluene may penetrate the WO_3 toplayer to contact with the TiO_2 layer. In this case, both WO_3 and TiO_2 are attributed to the photocatalytic reaction, resulting in a little higher photocatalytic activity than single WO_3 film.

3.3. Photocatalytic activity with a low bias

The application of an external bias voltage on the catalyst can draw the photo-generated electrons away via the external circuit, leaving the holes for mineralization of organic pollutants by their oxidation [37,38]. Therefore, compared to the unbiased photocatalytic process, the probability of the rapid recombination of electron–hole pairs in the PEC process can be reduced, and the photo-degradation ability can be enhanced. The processes that the electrons in the printed catalyst are driven to the external circuit by the biased interdigital electrode, has been reported in our previous work [25].

The observations in Section 3.2 indicate that the holes generated in the WO_3 are not sufficiently utilized for degrading the pollutants because of the suppression of the process 4. We believe that, when the electrons in the WO_3 could be further migrated to the external circuit (process 7), the recombination rate in the WO_3 layer would be reduced, and process 6 would be inhibited (as shown in Fig. 7c). Then, the process 4 can be smoothly operated, and the TiO_2 layer could obtain much more holes from the WO_3 layer. As a result, the photocatalytic activity of the S-W/T system could be further enhanced. To prove this hypothesis, a very low bias voltage of 0.2 V was applied on the interdigital electrode to draw the accumulated electrons of the WO_3 away via the external circuit.

Fig. 8 illustrates the dependence of C_t/C_0 with irradiation time over the S-T and S-W/T samples when 0.2 V bias is supplied. Surprisingly, the photocatalytic activity of S-W/T sample was enhanced markedly by applying a low bias voltage of 0.2 V. At this condition, the rate constant of S-W/T sample with 0.2 V bias was 5.2 times larger than that of S-T sample in the initial stage, and the evolved CO_2 was improved by 2.6 times (as shown in Table 2). It is also found that the reduced toluene is completely decomposed into CO_2, when the activity is obviously improved. As well, the results are consistent with the explanations in Fig. 7c.

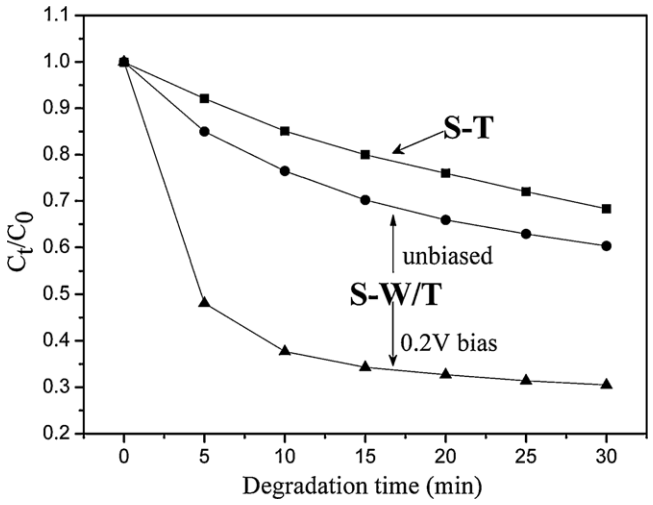

Fig. 8. Comparison of photocatalytic decomposition rates of toluene between S-T and S-W/T with no bias and 0.2 V bias.

Note that the S-T sample within pure TiO_2 film was not enhanced by applying a low bias voltage of 0.2 V (as shown in Table 2). Lately, Ye et al. found that the TiO_2 was applied with 82.5 V bias voltage, and the degradation rate constant could be raised as 1.26 times as TiO_2 without bias [24]. As can be seen, TiO_2 needs much higher bias than WO_3/TiO_2 coupled film to force the electrons away via external circuit. To explain this phenomenon, the photoelectric response of the S-T and S-W was measured (Fig. 9). Under the same bias voltage of 0.2 V, the photoelectric response of WO_3 is two to three orders of magnitude larger than that of TiO_2. In addition, we have noticed that the photoelectric response of TiO_2 rises abruptly to a maximum and then falls down to a steady state. However, the photoelectric response of WO_3 increases slowly, and the saturation of photocurrent is not attained in the testing process.

The effect of lower photoconductivity of TiO_2 is attributed to removal of conduction electrons by adsorbed O_2. It is well known that TiO_2 has a high potential of CB bottom (−4.21 eV versus Vacuum), so the free electrons have powerful reducibility. Oxygen molecules adsorbed on the TiO_2 surface could react with free electrons, creating negatively charged O_2^- ions [39]. Thereby, a depletion layer of electrons is created with low conductivity near the grain boundary. The energy supplied by the external bias voltage should be high enough to force the electrons to cross the electrons potential barrier. It can be concluded that the higher

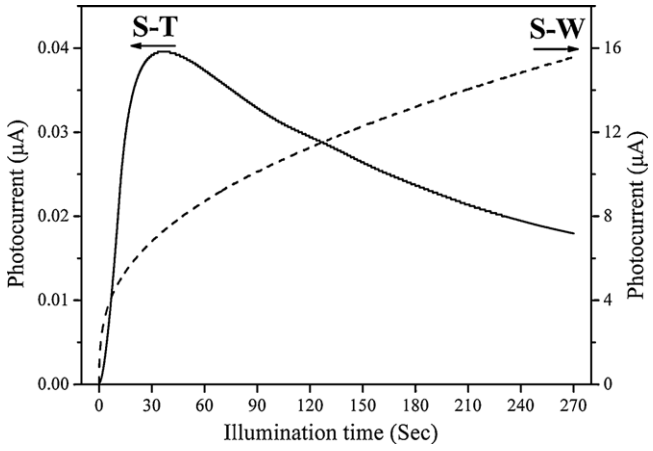

Fig. 9. Photocurrent–time testing curves of S-T and S-W samples during the UV-light illumination process adding 0.2 V bias in dry air.

Table 3
The photocurrent responses of different samples by application a bias voltage of 0.2, 0.5, 1, 2 V, respectively.

U (V)	S-T I (A)	S-W I (A)	S-T/W I (A)	S-W/T I (A)
0.2	4.0×10^{-8}	1.6×10^{-6}	1.1×10^{-7}	2.0×10^{-6}
0.5	1.1×10^{-7}	4.0×10^{-6}	3.6×10^{-7}	5.4×10^{-6}
1	3.1×10^{-7}	7.0×10^{-6}	7.4×10^{-7}	1.2×10^{-5}
2	9.2×10^{-7}	1.3×10^{-5}	3.5×10^{-6}	2.2×10^{-5}

U: bias voltage; I: photocurrent amplitude.

potential barrier is presented, and the higher bias is needed. In addition, the needed bias has the exponential growth with the height of potential barrier [40]. Thus the photocurrent of TiO_2 would fall down after reaching a maximum value. This is why a high bias is needed for pure TiO_2 to drive the electrons away and promote the degradation activity. Here, for the S-W/T sample, the photogenerated electrons in the CB of TiO_2 could be transferred to the CB of WO_3. Then, the electrons could be much easily driven to the external circuit through the WO_3 layer at a low voltage, which is an unimpeded conduction passageway for carrier transporting.

For this possibility, the photoelectric responses of different samples were measured by applying a bias voltage of 0.2, 0.5, 1, 2 V, respectively (as shown in Table 3). All the samples had relatively higher response amplitude by applying a higher bias voltage. Furthermore, the photoelectric response of WO_3 is much larger than that of TiO_2 at any bias voltage. The application of a larger bias voltage is mainly to enable the electron within the semiconductor across the barrier of the grain boundary between two crystals. However, it would hinder the practical application of the photocatalyst when the bias is too high. Therefore, the realization of low bias PEC degradation would promote the rapid development of this technology in practical application and meet the concept of low carbon economy.

3.4. Synergistic effect for charge separation combined with layered heterojunction and external low bias

In this study, it is demonstrated that the [interdigital electrode/WO_3/TiO_2] HEL system applied with a very low bias of 0.2 V can achieve remarkable improvement of gaseous pollutant photocatalysis compared with the single TiO_2 film. Both the interdigital electrode and the WO_3 layer play important roles in the HEL system. Either of them is indispensable for the multilevel separation of photoinduced electron–hole pairs as illustrated in Fig. 7c. Without the external bias, the holes generated in the WO_3 cannot be sufficiently utilized by the TiO_2 toplayer. Without the WO_3 layer, very high bias is needed for the single TiO_2 film to draw the electrons away via external circuit. Therefore, the [interdigital electrode/WO_3/TiO_2] HEL system combined with layered heterojunction and external low bias can generate a huge synergistic effect, resulting from strengthening the separation of the electron–hole pairs and showing a surface layer enriched with holes to react with the gaseous pollutants.

On the basis of the above experimental results, in order to distinctly define the HEL system, three functional layers are concluded as follows:

(1) TiO_2 as a wide bandgap semiconductor can generate photoinduced holes with a powerful oxidative ability. Under UV-light irradiation, the TiO_2 toplayer can enrich with holes from itself and the WO_3 layer to degrade the gaseous pollutants.
(2) WO_3 as a narrow bandgap semiconductor has an excellent electric conductivity and its CB and VB both lie under those of the TiO_2. Under UV and visible light irradiation, the WO_3 layer can

draw the electrons accumulated in its own CB and has potential to supply holes for the TiO_2 toplayer.

(3) Interdigital electrode is supplied with a low bias, and it can further separate the electrons in the WO_3 layer due to its good conductivity. This process can benefit the TiO_2 toplayer to obtain much more holes from the WO_3 underlayer.

4. Conclusion

In the presented work, the hole enriched in the surface of a material system was emphasized for photocatalysis in gas-phase. For this target, an ordered HEL system was proposed to get the holes sufficiently utilized. Furthermore, it was found that layered heterojunction and external low bias in our HEL system showed a huge synergistic effect by the suggested multilevel separation of photoinduced electron–hole pairs. The photocatalytic activity was remarkably improved in degrading the persistent toluene. Compared with the researches of mixed heterojuntion and single phase photoelectrocatalysis with high bias, the HEL system may supply some interesting enlightenments in gas-phase photocatalysis.

Acknowledgements

This work was supported by the Nature Science Foundation of China (No. 50927201) and the National Basic Research Program of China (Grant Nos. 2009CB939705 and 2009CB939702). The authors are also grateful to Analytical and Testing Center of Huazhong University of Science and Technology.

References

[1] X.B. Chen, S.H. Shen, L.J. Guo, S.S. Mao, Semiconductor-based photocatalytic hydrogen generation, Chem. Rev. 110 (2010) 6503–6570.
[2] U.G. Akpan, B.H. Hameed, Parameters affecting the photocatalytic degradation of dyes using TiO_2-based photocatalysts: a review, J. Hazard. Mater. 170 (2009) 520–529.
[3] W. Zhu, X. Liu, H.Q. Liu, D.L. Tong, J.Y. Yang, J.Y. Peng, Coaxial heterogeneous structure of TiO_2 nanotube arrays with CdS as a superthin coating synthesized via modified electrochemical atomic layer deposition, J. Am. Chem. Soc. 132 (2010) 12619–12626.
[4] M.H. Zhou, J.G. Yu, B. Cheng, Effects of Fe-doping on the photocatalytic activity of mesoporous TiO_2 powders prepared by an ultrasonic method, J. Hazard. Mater. 137 (2006) 1838–1847.
[5] A. Fujishima, X.T. Zhang, D.A. Tryk, TiO_2 photocatalysis and related surface phenomena, Surf. Sci. Rep. 63 (2008) 515–582.
[6] H.J. Huang, D.Z. Li, Q. Lin, W.J. Zhang, Y. Shao, Y.B. Chen, M. Sun, X.Z. Fu, Efficient degradation of benzene over $LaVO_4/TiO_2$ nanocrystalline heterojunction photocatalyst under visible light irradiation, Environ. Sci. Technol. 43 (2009) 4164–4168.
[7] Y.T. Kwon, K.Y. Song, W.I. Lee, G.J. Choi, Y.R. Do, Photocatalytic behavior of WO_3-loaded TiO_2 in an oxidation reaction, J. Catal. 191 (2000) 192–199.
[8] Y. Bessekhouad, D. Robert, J. Weber, Bi_2S_3/TiO_2 and CdS/TiO_2 heterojunctions as an available configuration for photocatalytic degradation of organic pollutant, J. Photochem. Photobiol. A 163 (2004) 569–580.
[9] X.P. Lin, J.C. Xing, W.D. Wang, Z.C. Shan, F.F. Xu, F.Q. Huang, Photocatalytic activities of heterojunction semiconductors $Bi_2O_3/BaTiO_3$: a strategy for the design of efficient combined photocatalysts, J. Phys. Chem. C 111 (2007) 18288–18293.
[10] M.V.B. Zanoni, J.J. Sene, H. Selcuk, M.A. Anderson, Photoelectrocatalytic production of active chlorine on nanocrystalline titanium dioxide thin-film electrodes, Environ. Sci. Technol. 38 (2004) 3203–3208.
[11] X. Zhao, J.H. Qu, H.J. Liu, C. Hu, Photoelectrocatalytic degradation of triazine-containing azo dyes at gamma-Bi_2MoO_6 film electrode under visible light irradiation lambda >420 Nm, Environ. Sci. Technol. 41 (2007) 6802–6807.
[12] X. Zhao, Y.F. Zhu, Synergetic degradation of rhodamine B at a porous $ZnWO_4$ film electrode by combined electro-oxidation and photocatalysis, Environ. Sci. Technol. 40 (2006) 3367–3372.
[13] W. Smith, Y.P. Zhao, Enhanced photocatalytic activity by aligned WO_3/TiO_2 two-layer nanorod arrays, J. Phys. Chem. C 112 (2008) 19635–19641.
[14] V. Keller, P. Bernhardt, F. Garin, Photocatalytic oxidation of butyl acetate in vapor phase on TiO_2, Pt/TiO_2 and WO_3/TiO_2 catalysts, J. Catal. 215 (2003) 129–138.
[15] J.H. Pan, W.I. Lee, Preparation of highly ordered cubic mesoporous WO_3/TiO_2 films and their photocatalytic properties, Chem. Mater. 18 (2006) 847–853.
[16] S. Biswas, M.F. Hossain, M. Shahjahan, K. Takahashi, T. Takahashi, A. Fujishima, Investigation of photocatalytic activity of TiO_2/WO_3 bilayered thin films with various amounts of WO_3 exposed surface, J. Vac. Sci. Technol. A 27 (2009) 880–884.
[17] S.Y. Chai, Y.J. Kim, M.H. Jung, A.K. Chakraborty, D. Jung, W.I. Lee, Heterojunctioned $BiOCl/Bi_2O_3$ a new visible light photocatalyst, J. Catal. 262 (2009) 144–149.
[18] Y. Tamaki, A. Furube, M. Murai, K. Hara, R. Katoh, M. Tachiya, Direct observation of reactive trapped holes in TiO_2 undergoing photocatalytic oxidation of adsorbed alcohols: evaluation of the reaction rates and yields, J. Am. Chem. Soc. 128 (2006) 416–417.
[19] Y.J. Kim, B. Gao, S.Y. Han, M.H. Jung, A.K. Chakraborty, T. Ko, C. Lee, W.I. Lee, Heterojunction of $FeTiO_3$ nanodisc and TiO_2 nanoparticle for a novel visible light photocatalyst, J. Phys. Chem. C 113 (2009) 19179–19184.
[20] B. Gao, Y.J. Kim, A.K. Chakraborty, W.I. Lee, Efficient decomposition of organic compounds with $FeTiO_3/TiO_2$ heterojunction under visible light irradiation, Appl. Catal. B 83 (2008) 202–207.
[21] N. Serpone, P. Maruhamuthu, P. Pichat, E. Pelizzetti, H. Hidaka, Exploiting the interparticle electron transfer process in the photocatalysed oxidation of phenol, 2-chlorophenol and pentachlorophenol: chemical evidence for electron and hole transfer between coupled semiconductors, J. Photochem. Photobiol. A 85 (1995) 247–255.
[22] J. Shang, S.D. Xie, T. Zhu, J. Li, Solid-state, planar photoelectrocatalytic devices using a manosized TiO_2 layer, Environ. Sci. Technol. 41 (2007) 7876–7880.
[23] Y.L. Xu, Y. He, X.D. Cao, D.J. Zhong, J.P. Jia, TiO_2/Ti rotating disk photoelectrocatalytic (PEC) reactor: a combination of highly effective thin-film PEC and conventional PEC processes on a single electrode, Environ. Sci. Technol. 42 (2008) 2612–2617.
[24] S.Y. Ye, Q.M. Tian, X.L. Song, S.C. Luo, Photoelectrocatalytic degradation of ethylene by a combination of TiO_2 and activated carbon felts, J. Photochem. Photobiol. A 208 (2009) 27–35.
[25] Y. Liu, C.S. Xie, H.Y. Li, H. Chen, Y.C. Liao, D.W. Zeng, Low bias photoelectrocatalytic (PEC) performance for organic vapour degradation using TiO_2/WO_3 nanocomposite, Appl. Catal. B 102 (2011) 157–162.
[26] P.S. Marcos, J. Marto, T. Trindade, J.A. Labrincha, Screen-printing of TiO_2 photocatalytic layers on glazed ceramic tiles, J. Photochem. Photobiol. A 197 (2008) 125–131.
[27] C.S. Xie, L.Q. Xiao, M.L. Hu, Z.K. Bai, X.P. Xia, D.W. Zeng, Fabrication and formaldehyde gas-sensing property of ZnO–MnO_2 coplanar gas sensor arrays, Sens. Actuators B 145 (2010) 457–463.
[28] M.H. Zhou, J.G. Yu, S.W. Liu, P.C. Zhai, B.B. Huang, Spray-hydrolytic synthesis of highly photoactive mesoporous anatase nanospheres for the photocatalytic degradation of toluene in air, Appl. Catal. B 89 (2009) 160–166.
[29] J.C. Yu, J.G. Yu, J.C. Zhao, Enhanced photocatalytic activity of mesoporous and ordinary TiO2 thin films by sulfuric acid treatment, Appl. Catal. B 36 (2002) 31–43.
[30] Z.J. Zou, Y. Liu, H.Y. Li, Y.C. Liao, C.S. Xie, Synthesis of $TiO_2/WO_3/MnO_2$ composites and high-throughput screening for their photoelectrical properties, ACS Comb. Sci. 12 (2010) 363–369.
[31] Y.C. Liao, H.Y. Li, Y.A. Liu, Z.J. Zou, D.W. Zeng, C.S. Xie, Characterization of photoelectric properties and composition effect of $TiO_2/ZnO/Fe_2O_3$ composite by combinatorial methodology, ACS Comb. Sci. 12 (2010) 883–889.
[32] S.F. Chen, L. Chen, S. Gao, G.Y. Cao, The preparation of coupled WO_3/TiO_2 photocatalyst by ball milling, Powder Technol. 160 (2005) 198–202.
[33] M.A. Butler, D.S. Ginley, Prediction of flatband potentials at semiconductor–electrolyte interfaces from atomic electronegativities, J. Electrochem. Soc. 125 (1978) 228–232.
[34] R. Abe, H. Takami, N. Murakami, B. Ohtani, Pristine simple oxides as visible light driven photocatalysts: highly efficient decomposition of organic compounds over platinum-loaded tungsten oxide, J. Am. Chem. Soc. 130 (2008) 7780–7781.
[35] H. Yu, S. Chen, X. Quan, H. Zhao, Y. Zhang, Fabrication of a TiO_2–BOD heterojunction and its application as a photocatalyst for the simultaneous oxidation of an azo dye and reduction of Cr(VI), Environ. Sci. Technol. 42 (2008) 3791–3796.
[36] K.M. Schindler, M. Kunst, Charge-carrier dynamics in TiO_2 powders, J. Phys. Chem. 94 (1990) 8222–8226.
[37] Z.H. Zhang, Y. Yuan, G.Y. Shi, Y.J. Fang, L.H. Liang, H.C. Ding, L.T. Jin, Photoelectrocatalytic activity of highly ordered TiO_2 nanotube arrays electrode for azo dye degradation, Environ. Sci. Technol. 41 (2007) 6259–6263.
[38] X.Z. Li, H.L. Liu, P.T. Yue, Y.P. Sun, Photoelectrocatalytic oxidation of rose bengal in aqueous solution using a Ti/TiO_2 mesh electrode, Environ. Sci. Technol. 34 (2000) 4401–4406.
[39] F. Guzman, S.S.C. Chuang, Tracing the reaction steps involving oxygen and IR observable species in ethanol photocatalytic oxidation on TiO_2, J. Am. Chem. Soc. 132 (2010) 1502–1503.
[40] A. Varpula, S. Novikov, J. Sinkkonen, M. Utriainen, Bias dependent sensitivity in metal-oxide gas sensors, Sens. Actuators B 131 (2008) 134–142.